Research Article Vol. 26, No. 20 | 1 Oct 2018 | OPTICS EXPRESS 25934

Optics EXPRESS

120 Gbaud PAM-4 transmission over 80-km SSMF using optical band interleaving and Kramers-Kronig detection

TAO GUI,[1,2] LANGYU YI,[1,3] CHANGJIAN GUO,[1,3,*] CHAO LU,[3] AND ALAN PAK TAO LAU[2]

[1]*MOE International Laboratory for Optical Information Technologies, South China Academy of Advanced Optoelectronics, South China Normal University, Guangzhou 510006, China*
[2]*Photonics Research Centre, Department of Electrical Engineering, The Hong Kong Polytechnic University, Hung Hom, Kowloon, Hong Kong, China*
[3]*Photonics Research Centre, Department of Electronic and Information Engineering, The Hong Kong Polytechnic University, Hung Hom, Kowloon, Hong Kong, China*
[*]*changjian.guo@coer-scnu.org*

Abstract: We demonstrate generation and detection of 120-Gbaud PAM-4 signals using an I/Q modulator based on optical band interleaving (OBI) technique. The spectral components of target PAM signals are split and pre-processed before being sent to two digital-to-analog convertors (sub-DACs) whose outputs are imprinted to an optical carrier by an optical I/Q modulator forming a carrier-suppressed tandem single side-band (SSB) signal. The PAM signals can be recovered after photo-detection provided that an optical beating tone is added at the edge of the signal spectrum along with the modulator output. The proposed method requires only half of the Nyquist bandwidth of the target PAM signal for the transmitter and has the advantage of a simple implementation. Using Kramers-Kronig (K-K) detection, a 120 Gbaud PAM-4 transmission over 80-km standard single mode fiber (SSMF) is successfully demonstrated. The proposed scheme entails a simple implementation and a much lower bandwidth requirement at the transmitter compared with conventional all-electronic high baud rate signal generation schemes.

OCIS codes: (060.2330) Fiber optics communications, (060.4080) Modulation.

References and links

1. K. Zhong, X. Zhou, T. Gui, L. Tao, Y. Gao, W. Chen, J. Man, L. Zeng, A. P. T. Lau, and C. Lu, "Experimental study of PAM-4, CAP-16, and DMT for 100 Gb/s short reach optical transmission systems," Opt. Express **23**(2), 1176–1189 (2015).
2. T. Richter, E. Palushani, C. S. Langhorst, R. Ludwig, L. Molle, M. Nölle, and C. Schubert, "Transmission of single-channel 16-QAM data signals at Terabaud symbol rates," J. Lightwave Technol. **30**(4), 504–511 (2012).
3. R. Rios-Muller, J. Renaudier, P. Brindel, H. Mardoyan, P. Jenneve, L. Schmalen, and G. Charlet, "1-terabit/s net data-rate transceiver based on single-carrier Nyquist-shaped 124 GBaud PDM-32QAM," in Optical Fiber Communication Conference (Optical Society of America, 2015), Paper Th5B.1.
4. J. Zhang, J. Yu, and H.-C. Chien, "Advanced algorithm for high-baud rate signal generation and detection," in Optical Fiber Communication Conference (Optical Society of America, 2017), paper M3D.1.
5. X. Chen, S. Chandrasekhar, S. Rande, G. Raybon, A. Adamiecki, P. Pupalaikis, and P. Winzer, "All-electronic 100-GHz bandwidth digital-to-analog converter generating PAM signals up to 190-GBaud," in Optical Fiber Communication Conference (Optical Society of America, 2016), paper Th5C.5.
6. H. Yamazaki, M. Nagatani, F. Hamaoka, S. Kanazawa, H. Nosaka, T. Hashimoto, and Y. Miyamoto, "300-Gbps discrete multi-tone transmission using digital-preprocessed analog-multiplexed DAC with halved clock frequency and suppressed Image," *in Proceedings of European Conference on Optical Communication* (Institute of Electrical and Electronics Engineers, 2014), post deadline paper.
7. X. Chen, S. Chandrasekhar, P. Pupalaikis, and P. Winzer, "Fast DAC solutions for future high symbol rate systems," in Optical Fiber Communication Conference (Optical Society of America, 2017), paper Tu2E.3.
8. Y. Zhang, M. O'Sullivan, and R. Hui, "Theoretical and experimental investigation of compatible SSB modulation for single channel long-distance optical OFDM transmission," Opt. Express **18**(16), 16751–16764 (2010).
9. A. Mecozzi, C. Antonelli, and M. Shtaif, "Kramers–Kronig coherent receiver," Optica **3**(11), 1220–1227 (2016).

#334697 https://doi.org/10.1364/OE.26.025934
Journal © 2018 Received 7 Jun 2018; revised 8 Aug 2018; accepted 9 Aug 2018; published 20 Sep 2018

10. A. Mecozzi, C. Antonelli, and M. Shtaif, "A necessary and sufficient condition for minimum phase and implications for phase retrieval," arXiv preprint arXiv:1606.04861 (2016).
11. X. Chen, C. Antonelli, S. Chandrasekhar, G. Raybon, A. Mecozzi, M. Shtaif, and P. Winzer, "Kramers–Kronig receivers for 100-km datacenter interconnects," J. Lightwave Technol. **36**(1), 79–89 (2018).
12. S. T. Le, K. Schuh, M. Chagnon, F. Buchali, R. Dischler, V. Aref, H. Buelow, and K. Engenhardt, "1.72-Tb/s virtual-carrier-assisted direct-detection transmission over 200 km," J. Lightwave Technol. **36**(6), 1347–1353 (2018).
13. C. Antonelli, A. Mecozzi, and M. Shtaif, "Kramers-Kronig PAM transceiver," in Optical Fiber Communication Conference (Optical Society of America, 2017), paper Tu3I.5.
14. C. Antonelli, A. Mecozzi, and M. Shtaif, "Kramers-Kronig PAM transceiver and two-side polarization-multiplexed Kramers-Kronig transceiver," J. Lightwave Technol. **36**(2), 468–475 (2018).
15. T. M. Hoang, M. Y. S. Sowailem, Q. Zhuge, Z. Xing, M. Morsy-Osman, E. El-Fiky, S. Fan, M. Xiang, and D. V. Plant, "Single wavelength 480 Gb/s direct detection over 80 km SSMF enabled by Stokes vector Kramers Kronig transceiver," Opt. Express **25**(26), 33534–33542 (2017).
16. T. Bo and H. Kim, "Kramers-Kronig receiver operable without digital upsampling," Opt. Express **26**(11), 13810–13818 (2018).

1. Introduction

Rapid traffic growth in data centers requires the use of high-capacity intra- and inter- data center optical interconnects, which calls for next generation optical interfaces of 800 GE or even 1.6 TbE. In typical data center applications, direct detection (DD) is still preferred over coherent detection due to its lower cost, smaller footprint and lower power consumption. Meanwhile, single lambda, single polarization PAM-4 signaling beyond 100 Gbaud is a key technology for future 800 GE interfaces enabling an increase in system capacity while decreasing the number of electrical and optical components [1]. For generating signals with baud rates higher than 100 Gbaud, various techniques have been proposed. Optical frequency synthesis [2] and optical time-division multiplexing [3] techniques have been employed in laboratory settings to generate high-bandwidth signals. In [4], 128.8 Gbaud 16-QAM signal generation is reported using multi-stage electrical multiplexers. On the other hand, in [5], 195 Gbaud PAM-4 generation based on a 100-GHz DAC with digital band interleaving (DBI) is demonstrated. Also, Yamazaki *et al*. [6], demonstrated 300-Gbps digital multitone (DMT) transmission using a digital-preprocessed analog-multiplexed DAC. A more detailed review can be found in [7]. Among existing techniques, all-electronic high-symbol-rate generation schemes feature a simple modulation structure since they require only one single optical modulator to imprint the modulating signal onto a single laser carrier, as shown in Fig. 1. However, these schemes usually require delicate and complex electrical setups and/or large-bandwidth electrical and optical components.

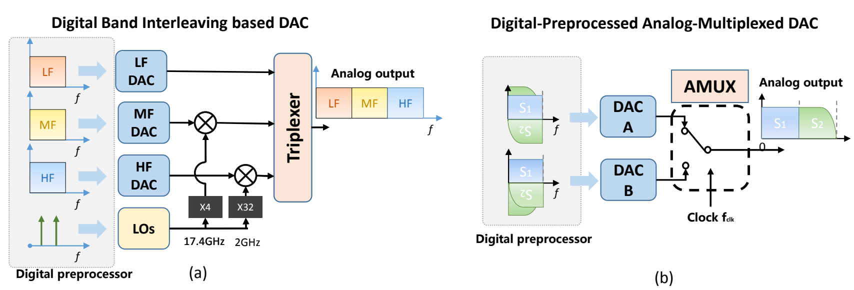

Fig. 1. Recently-proposed all-electronic high-symbol-rate generation schemes. (a) DBI based DAC [5]; (b) Digital-preprocessed analog-multiplexed DAC [6].

Another limiting factor for high speed DD systems in C-band is the power fading problem induced by chromatic dispersion (CD). SSB modulation is a commonly used technique that can effectively mitigate the effects of CD. However, it suffers from signal-signal beat interference (SSBI) caused by square-law detection [8]. Thanks to the recently proposed Kramers-Kronig (K-K) scheme [9], the complex optical field can be reconstructed from the

Optics EXPRESS

photo-detected amplitude waveform using the K-K relationship provided that the signal meets the minimum phase condition. The K-K scheme avoids SSBI and provides a low-complexity, power-efficient solution for SSB/DD systems. The K-K based PAM transceivers were firstly proposed in [13] and a two-sided polarization multiplexed K-K transceiver was proposed in [14] where the two-sided SSB signals were de-interleaved and processed in parallel.

In this paper, we propose an I/Q modulator based optical band interleaving (OBI) technique to generate SSB PAM-4 signals of up to 120 Gbaud using commercially available components with only ~30 GHz analog bandwidth at the transmitter, thus entailing a simple structure and a lower bandwidth requirement at the transmitter compared with the existing all-electronic high baud rate signal generation schemes. Based on the proposed OBI technique, 120-Gbaud PAM-4 SSB/DD transmission over 80 km SSMF is successfully demonstrated with K-K based direct detection. Regarding implementation aspects, an optical carrier (i.e. an additional laser source) and a virtual (digital) carrier are utilized as the beating tone of the SSB signals. We experimentally show that though the virtual carrier-based schemes have much simpler implementation, an additional OSNR penalty is observed due to the SNR reduction of the generated PAM-4 signals.

2. Principle of the OBI based PAM generation and detection

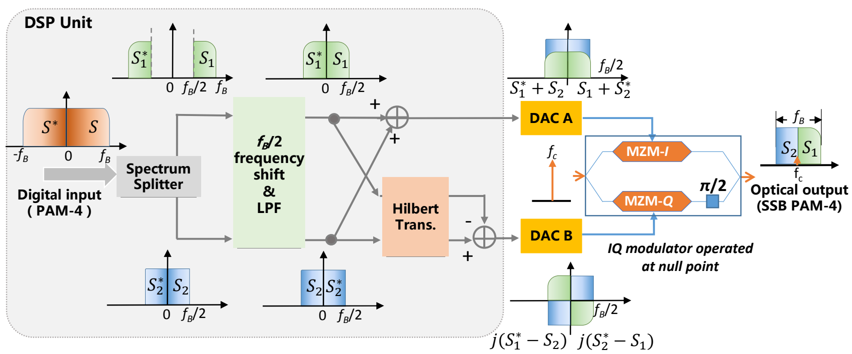

Fig. 2. Principle of the OBI PAM-4 waveform generator.

Figure 2 schematically shows the operating principle of the proposed OBI based PAM-4 signal generator. The signal generator consists of a digital pre-processor, two sub-DACs and an optical I/Q modulator. Here, we assume that the digital input signal $S(t)$ is a PAM-4 signal with a bandwidth slightly smaller than f_B while the analog bandwidths of sub-DACs and I/Q modulator are constrained within $f_B/2$. The spectrum of PAM-4 signal $S(t)$ can be expressed as $S = S^*(-f) + S(f)$, where $S(f)$ represents the positive single side-band spectrum. In the pre-processing unit, the signal spectrum is firstly split into two parts i.e. lower frequency components $S_2 = S_2^*(-f) + S_2(f)$ and higher frequency components $S_1 = S_1^*(-f) + S_1(f)$. The two frequency components are then shifted by $f_B/2$ and bandlimited to $f_B/2$ using an ideal low pass filter. Next, the shifted S_1 and S_2 are added and sent to the sub-DAC A as

$$S_{\text{DAC-A}} = S_1^*\left(-f + \frac{f_B}{2}\right) + S_1\left(f + \frac{f_B}{2}\right) + S_2^*\left(-f + \frac{f_B}{2}\right) + S_2\left(f + \frac{f_B}{2}\right). \tag{1}$$

Meanwhile, their duplications are Hilbert transformed and then combined to generate the signals to be sent to the sub-DAC B, which can be written as:

$$S_{\text{DAC-B}} = \left\{ S_1^* \left(-f + \frac{f_B}{2} \right) - S_1 \left(f + \frac{f_B}{2} \right) - S_2^* \left(-f + \frac{f_B}{2} \right) + S_2 \left(f + \frac{f_B}{2} \right) \right\} e^{\frac{\pi}{2} j}. \quad (2)$$

The electrical waveforms $S_{\text{DAC}-\text{A}}$ and $S_{\text{DAC}-\text{B}}$ are then amplified to drive an optical I/Q modulator biased at null point. The optical output signal can be approximated as

$$E_{out}(f) \approx S_1 \left(f - f_c + \frac{f_B}{2} \right) + S_2 \left(f - f_c + \frac{f_B}{2} \right) = S \left(f - f_c + \frac{f_B}{2} \right). \quad (3)$$

One can easily observe from (3) that after optical modulation, the S_1 and S_2 signal bands are converted to optical SSB signal beside the left and right side of carrier frequency f_c, respectively. Therefore, the whole band of the modulated optical signal is the reconstruction of the target signal in the optical field. It should be noted that in practical applications, the laser has a certain linewidth and the residual optical carrier after the optical I/Q modulator exists due to limited extinction ratio. The residual optical carrier may degrade SNR of the received PAM signals. In such circumstances, a guard band of $2 \times f_g$ can be applied to S_1 and S_2 by modifying their shifting frequency to $f_B/2 - f_g$ and $f_B/2 + f_g$, respectively. At the receiver, this guard band is discarded and another frequency shift of $2 \times f_g$ can be applied to S_1 to reconstruct the original PAM signal. In this way, the impact of residual carrier on the signal can be reduced. Figure 4(b) depicts the simulated BER as a function of extinction ratio (ER) of the optical IQ modulator with and without guard band. The linewidth of the laser is 100 KHz, and the received SNR is 21 dB. Clearly, adding a guard band significantly improves the BER performance, especially when the ER is smaller than 25 dB.

After combining an optical tone with the generated optical SSB signal, the complex optical field signal in time domain before the photodiode (PD) can be expressed as:

$$E_{out}(t) \approx \left[A + s(t) + j\hat{s}(t) \right] e^{j2\pi \left(f_c - \frac{f_B}{2} \right) t}. \quad (4)$$

The detected electrical signal after PD can be written as:

$$I(t) = \left| E_{out}(t) \right|^2 = A^2 + 2A \cdot s(t) + \underbrace{\left| s(t) \right|^2 + \left| \hat{s}(t) \right|^2}_{SSBI}, \quad (5)$$

which contains a DC component A^2, the signal of interes $s(t)$, and the SSBI component $|s(t)|^2 + |\hat{s}(t)|^2$ that falls in-band and thus causes performance degradation [as shown in Fig. 3(a)]. Development of algorithms and techniques which can combat SSBI effects has been an active research area over the last few years. Among the proposed methods, K-K based field reconstruction scheme is a promising solution [9]. By using the K-K relationship, one can reconstruct the full complex received optical field from the beating of the signal spectrum with a co-propagating tone at the edge of the signal spectrum. This tone does not have to be locked in frequency or phase to the signal and can be generated either electronically together with the signal or optically through a wavelength shifter. The success of digital signal processing (DSP) aided optical field re-construction relies on the condition that the detected optical signal must be *minimum-phase*. When this condition is satisfied, the phase information can be obtained from the magnitude spectrum via Hilbert transform [9]. To satisfy minimum-phase condition, the carrier-to-signal power ratio (CSPR) should be large enough. Details of the K-K principle can be found in [9,10]. The block diagram of K-K receiver algorithm is illustrated in Fig. 3(b).

Optics EXPRESS

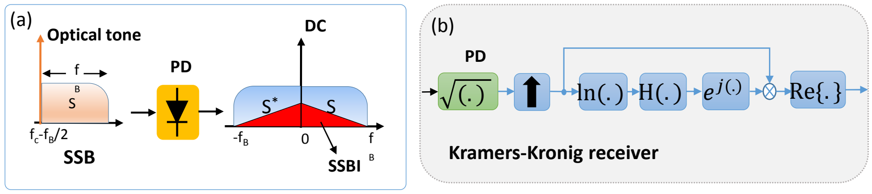

Fig. 3. (a) The spectra of PAM-4 SSB signals before and after PD; (b) block diagram of K-K PAM receiver.

We conducted a simulation under AWGN to analyse the receiver sensitivity of the proposed 120 Gbaud PAM-4 SSB/DD systems with and without using K-K. The simulation parameters are ideal and the BER results as a function of effective SNR are depicted in Fig. 4(a). The effective SNR is defined as the ratio of the signal power (excluding the optical tone) to the in-band noise power. The empty markers represent the case of without using K-K whereas the filled markers represent the case where K-K has been used. Compared with the theoretical curve, the K-K based detection scheme shows an excellent performance with < 0.2 dB SNR penalty at a CSPR of 11 dB (at a BER of 1E-4).

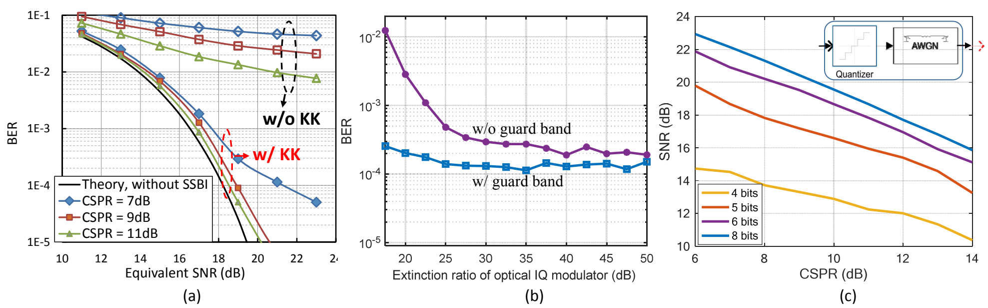

Fig. 4. (a) Simulation results showing receiver sensitivity of 120 Gaud PAM-4 SSB systems with and without K-K under different CSPRs; (b) Simulated BER as a function of the extinction ratio (ER) of the optical I/Q modulator at a SNR of 21 dB. The laser linewidth was 100 KHz. (c) The electrical SNR of the generated PAM-4 signal as a function of the CSPR in VC cases.

3. Experimental setup

Figure 5 shows the experimental setup and the receiver DSP structure of our proposed scheme. The 120 Gbaud PAM-4 signals were firstly spectral shaped using a root raised-cosine (RRC) filter with a roll off factor of 0.05, and pre-processed offline according to Fig. 2. The resulting two sub-band waveforms were loaded into a 90-Gsa/s arbitrary waveform generator (AWG, Keysight M8196A, 32-GHz bandwidth) to produce the electrical signals, which were then amplified and sent to an optical I/Q modulator (Fujitsu FTM7961, with a 3-dB bandwidth of about 26 GHz) to generate the optical carrier-suppressed tandem SSB signal. An external cavity laser (ECL #1) with a linewidth of around 100 kHz and a centre wavelength of 1550.12 nm was used as an optical carrier. Two schemes to generate the co-propagating optical tone needed by direct detection at the receiver were investigated. The first one simply used an additional optical carrier (ECL #2) with its centre frequency shifted by > 30 GHz from ECL #1, as shown in Fig. 5(a). The optical SSB signal and the optical carrier were then combined using a coupler and sent to a spool of 80-km SSMF. It should be noted that additional frequency offset estimation (FOE) and carrier phase estimation (CPE) should be applied at the receiver if two free running lasers are used [11]. However, both FOE and CPE can be done using an electrical pilot tone generated along with the PAM signals. The other scheme was to generate a large-power digital carrier (virtual carrier, VC) at the edge of the S_1 together with the information-bearing signals, as shown in Fig. 5(b). Compared with the optical approach, this scheme can significantly decrease the implementation cost since the additional laser and the extra FOE/CPE algorithms are omitted.

The downside of the VC scheme, however, is that it suffers a significant SNR loss of the PAM-4 signals after DACs [12]. This is because a large part of signal power is occupied by the virtual carrier for generating the optical tone to maintain a certain CSPR (around 10 dB), and the effective number of bits (ENOB) of the DACs are limited. This phenomenon is illustrated in the simulation results shown in Fig. 4(c). The DAC here is modeled by a quantizer (with its ENOB varies from 4 to 8 bits) cascaded with an AWGN (with an intrinsic SNR of 30 dB) channel, as shown in the inset of Fig. 4(c). The simulated SNRs are calculated from the output of the DAC after removing the virtual carrier using an ideal lowpass filter. From Fig. 4(c), the following observations could be made: 1) A larger ENOB can bring a larger SNR, which is only natural since the quantization noise is reduced when a large ENOB is used. 2) the electrical SNR of the signal drops dramatically as the CSPR increases. When the CSPR reaches 11 dB, which is observed to be the optimum value in our experiments, the achievable electrical SNR is only 16 dB using an ENOB of 6 bits (state-of-the-art high-speed DACs typically have an ENOB of 5 ~6 bits).

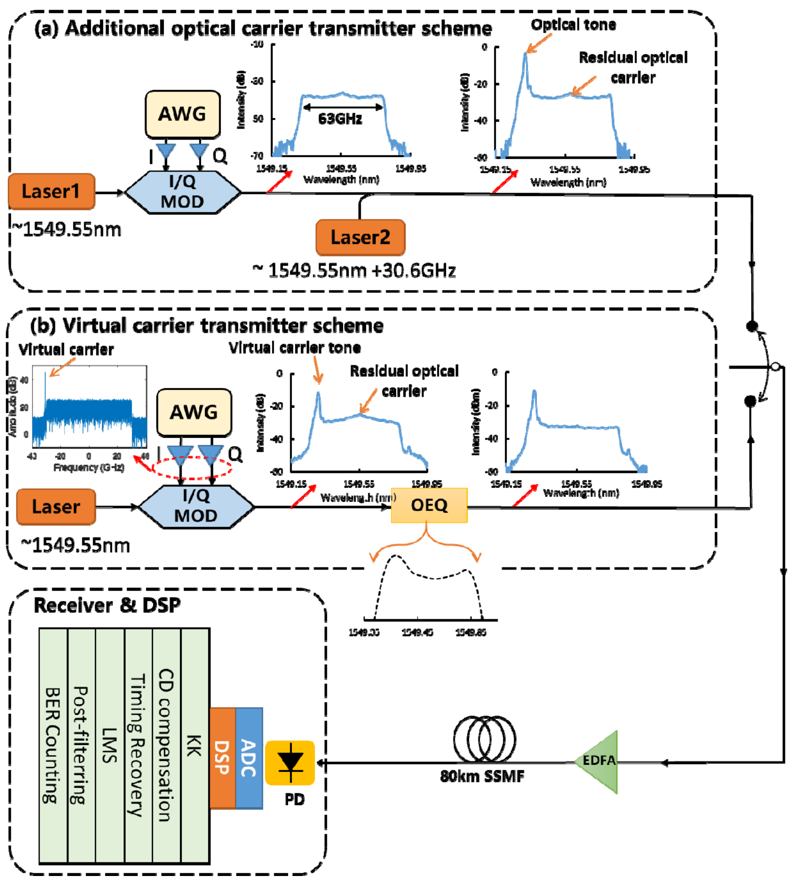

Fig. 5. Experimental setup of the OBI based 120 Gbaud PAM-4 SSB/DD system and its DSP structure. (a) additional optical carrier (AOC) transmitter scheme; (b) virtual carrier (VC) transmitter scheme. (MOD: modulator; EDFA: erbium-doped fiber amplifier).

Another constraint of the VC assisted K-K scheme is the reduction of optical power for the PAM-4 signal after I/Q modulation, since the VC and PAM-4 signal are modulated simultaneously onto one optical carrier, leading to a limited OSNR. This constraint can be overcome by using optical amplifiers. The process of the OEQ is depicted in the Fig. 5. We firstly generate the SSB PAM-4 signal with a relatively small virtual carrier, whose optical spectra after I/Q modulator is shown in the inset of Fig. 5(b). Note that the CSPR for now is not enough to the K-K receiver. Secondly, the modulated signals are amplified using an EDFA to boost the optical power. A specially designed OEQ filter is then used so that the spectra of the PAM-4 signal are slightly suppressed while the virtual carrier keeps invariant. In this way, the CSPR is increased, at the expanse of a reduction of the OSNR. Note that from the experimental results shown in Figs. 6(a) and 6(d), one can conclude that the limited electrical SNR is the main reason for the performance degradation in our experiment. Obviously, by generating the SSB PAM-4 signal with a smaller virtual carrier, we may have a higher electrical SNR for the PAM-4 signal spectrum. This gain in the electrical SNR is more significant than the loss of the OSNR, since it can be compensated using optical amplifiers. In this way, both values of SNR and CSPR can be increased after the OEQ. The use of OEQ enables us to improve the SNR of the PAM-4 signal while maintaining a certain CSPR, since the K-K receiver requires the CSPR to be large enough so that the minimum-phase condition is satisfied.

At the receiver, a single PD (with a 3-dB bandwidth of 100 GHz) was used in conjunction with a 62 GHz real-time oscilloscope. Apparently, the AWG, optical I/Q modulator and the real-time scope all pose a bandwidth limit to our system as the actual bandwidth of the target PAM-4 signal is more than 63 GHz (using an RRC shaping filter with a roll off factor of 0.05). Therefore, despite the fact pointed out by [15] that a few GHz of guard band between the carrier and the signal can have some benefits in terms of receiver SNR, the allowable guard band between the optical/virtual carrier and the PAM-4 signal in this work is very limited since further increasing the guard band would lead to a dramatic performance degradation due to bandwidth limitation of the devices. In fact, the guard band was set to be 600 MHz in VC cases. The sampled signal was analyzed off-line using DSP whose structure is also shown in Fig. 5. The DSP procedures include: 1) digital up-sampling to 240 Gsa/s to produce a signal with 2-samples/symbol; 2) optical phase retrieval and complex signal reconstruction using the K-K relationship; 3) optional pilot-based FOE and CPE when an additional optical carrier was used as the beating tone; 4) frequency domain equalization (FDE) based CD compensation; 5) feed-forward timing phase estimation (TPE); 6) decision-directed least mean square (DD-LMS) linear equalization, demodulation, and BER counting.

4. Results and discussions

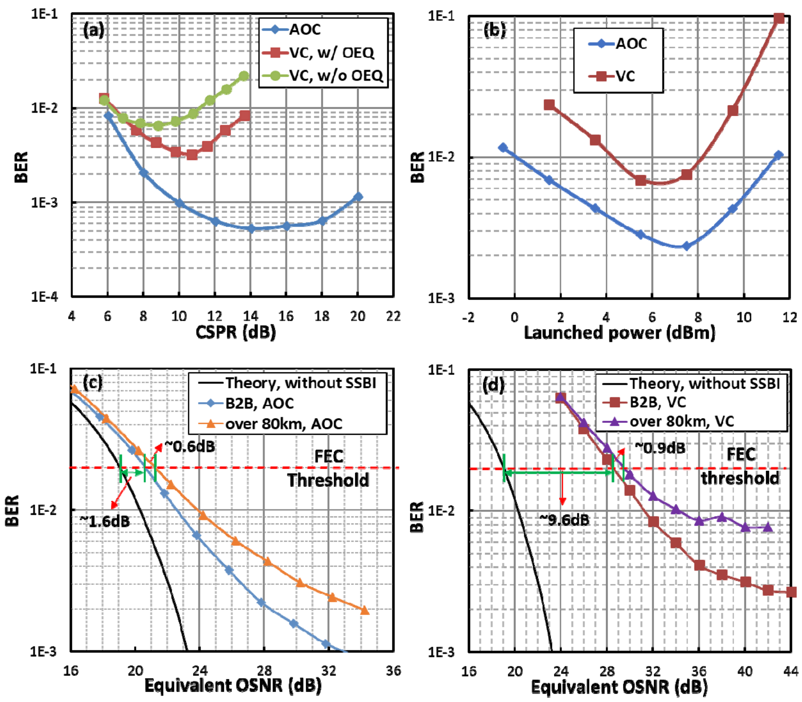

Fig. 6. (a) BER as a function of CSPR in back-to-back (B2B) case; (b) Optimization of launched power for 80 km transmission under optimum CSPR; The measured BER vs. equivalent OSNR for (c) AOC scheme and (d) VC scheme, under B2B and 80-km transmission cases. The black curves show theoretical BER performance of the PAM-4 signals under AWGN without SSBI.

The optimization results of CSPR in B2B scenario for both AOC and VC transmitter schemes are shown in Fig. 6(a). The following observations could be made: 1) For AOC case (i.e. blue line), the optimum CSPR is found to be around 14 dB, while a BER floor exists when CSPR varies from 12 to 18 dB; 2) For VC cases with and without OEQ, however, the optimum CSPR values are 11 dB and 9 dB, respectively; 3) The BER performance can be effectively improved when an OEQ is used [red curve in Fig. 6(a)] in VC cases. Obviously, the AOC scheme significantly outperforms the VC scheme. The reason is that the SNR of the PAM signal generated using a VC transmitter is smaller than that generated using an AOC transmitter since a large portion of the electrical power is allocated for the generation of the VC. However, an OEQ can be used to boost the SNR of the PAM signal while maintaining a certain value of CSPR, thus resulting in a significant performance improvement. Based on the optimum CSPR obtained from Fig. 6(a), we tested different launched optical powers to get the minimum BER over 80-km SSMF transmission, as shown in Fig. 6(b). The results show that the optimal launched power is around 7 dBm for both AOC and VC schemes. In Fig. 6(c) and 6(d), we plot BER as a function of the equivalent OSNR for both schemes. The equivalent OSNR is the OSNR one would measure in the absence of the optical carrier [9]. In AOC cases, the equivalent OSNR was obtained by simply measuring the OSNR of the optically modulated signal before combining the AOC. In VC cases, the measurement of the equivalent OSNR is a two-step process. Firstly, we measure the power of one half of the signal spectra without the virtual tone, denoted as P_h. The power of the optical signal is therefore $2 \times P_h$. The power of the ASE noise, denoted as N_{ASE}, is measured in a 0.1 nm window. Then, the equivalent OSNR is $(2\times P_h)/N_{ASE}$. At the 20% soft decision forward error correction (SD-FEC) threshold with a BER of 2E-2, the OSNR penalty for the AOC scheme is ~1.6 dB in comparison with the theoretical curve while after transmission over 80 km SSMF, an additional ~0.6 dB OSNR penalty is observed.

The error floor in Fig. 6(c) is caused by the limited electrical SNR of the signals generated from the AWG. The RF pilot-based carrier phase estimation (CPE) used in AOC cases may also contribute to the OSNR penalty. Meanwhile, one can see from the results of the VC scheme shown in Fig. 6(d) that after 80-km SSMF transmission, a large error floor of about 7E-3 can be found when the equivalent OSNR is larger than 36 dB. The reason is as follows: For the VC assisted K-K detection, the electrical SNR of the generated PAM-4 spectrum is affected by the power of the VC, and the ENOB of the DAC, as shown in Fig. 4(c). Meanwhile, the optical SNR of the modulated signals is also limited since both the VC and the PAM-4 signal are modulated simultaneously using a single optical modulator. As mentioned in section 3, the SNR and the CSPR can both be improved by using an OEQ, while the optical SNR can be boosted using an EDFA. The fact from Fig. 6(d) that different error floors exist for both B2B and 80-km cases indicates that increasing the OSNR cannot lead to a better BER. Therefore, the insufficient electrical SNR is the key issue. Also, for 80-km SSMF transmission, an additional EDFA was used at the transmitter to boost the optical power to around 7 dBm before it was launched into the SSMF. The added amplified spontaneous emission (ASE) noise may further compromise the signal SNR. One can see that the OSNR penalty after 80 km transmission is still within 1 dB at the BER of 2E-2. However, the implementation penalty in comparison with the theoretical curve is increased to ~9.6 dB. Thus, a tradeoff between performance and implementation cost needs to be considered.

As [9] pointed out, digital upsampling before a K-K algorithm is needed to enhance the system performance due to the spectrum broadening caused by the nonlinear operations such as logarithm and exponential functions. A modified K-K algorithm without the need of upsampling is also proposed in [16]. However, it should be noted that neither of the above-mentioned schemes may help in improving our system's performance. The reason for this discrepancy might be the bandwidth limitations of the AWG as well as the real time scope, which dominate the error magnitude spectra as shown in Fig. 7. The error magnitude spectra have three peaks, located near DC, at the center (30 GHz), and at around 60 GHz, respectively. Apparently, the two peaks at DC and 60 GHz are caused by the bandwidth limitations of the AWG and the scope. These two peaks are also much larger than that at round 30 GHz which is caused by the residual optical carrier. We therefore conclude that the dominant noise source of this experiment arises from the bandwidth limitations and using a guard band between the frequency components S_1 and S_2 might not help much to improve the performance.

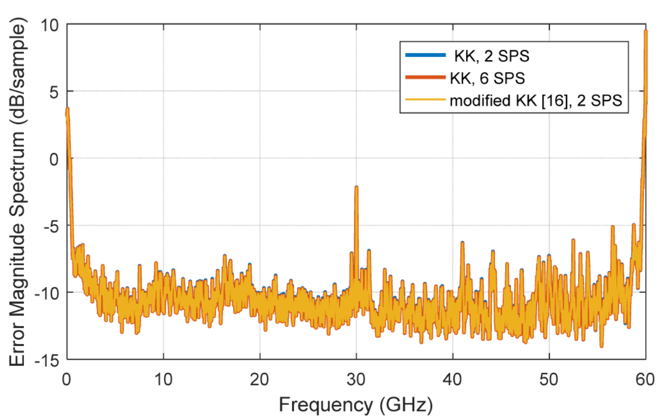

Fig. 7. Error magnitude spectra after decision-directed least-mean-square (DD-LMS) equalization with different K-K schemes.

5. Summary

In this paper, we proposed a simple and bandwidth friendly method for high baud rate PAM generation and detection based on an optical band interleaving technique. The proposed scheme combines the spectral components of the PAM signals optically using a single optical I/Q modulator, thus eliminating the need for delicate tuning of the optical and electrical devices. Also, only half of the Nyquist bandwidth of the target PAM signal is needed for the transmitter. Using two DACs and an optical I/Q modulator with less than 30 GHz bandwidth at the transmitter, a single-channel 240 Gb/s PAM-4 generation and transmission has been successfully demonstrated using K-K receiver-based DD over 80 km SSMF. Two methods have been applied to add the beating tone along with the generated optical tandem SSB signals. The VC based scheme has the merit of simple implementation, however, it suffers from a significant OSNR penalty compared with the AOC based scheme.

Funding

Pearl River S&T Nova Program of Guangzhou (201710010028) and Hong Kong Government General Research Fund (PolyU 152079/14E).

Acknowledgments

The authors wish to acknowledge their gratitude to Dr. Faisal Nadeem Khan from the Hong Kong Polytechnic University for his help and fruitful discussion.